Quantum simulation of the heat capacity of water

Wataru Shinoda[1,*] and Motoyuki Shiga[2,†]

[1]*Research Institute for Computational Sciences (RICS), National Institute of Advanced Industrial Science and Technology (AIST), Central 2, 1-1-1, Umezono, Tsukuba, Ibaraki 305-8568, Japan*

[2]*Center for Promotion of Computational Science and Engineering, Japan Atomic Energy Research Institute, 6-9-3, Higashi-Ueno, Taito-ku, Tokyo 110-0015, Japan*

(Received 18 November 2004; published 22 April 2005)

Path integral molecular dynamics simulations have been carried out to evaluate heat capacities of water in gas, liquid, and solid phases. For convergence, a 100-ps simulation run with a large path integral variable ($P \sim 128$) was required even by using the double-centroid virial heat capacity estimator. For all states, the quantum corrections to the heat capacities are significantly large. The calculated heat capacities for vapor and ice I_h agreed excellently with experimental data, while that for liquid was less than the experimental value by $\sim$20% due to the limit of the SPC/F potential model.

DOI: 10.1103/PhysRevE.71.041204 PACS number(s): 65.20.+w, 02.70.Ns, 65.40.−b

Quantitative estimation of the heat capacity in liquids and solids has been a difficult issue in molecular simulations. This is because, as found by Einstein [1], heat capacity involves the quantum mechanics of atomic vibrations, especially at temperatures below the Debye temperature. Quantum effects are also important for the heat capacity of gas-phase molecules if the energy increment between the vibrational (rotational) states is larger than kT. (Actually, the reason that the molecules are usually treated as rigid rotors in calculating the heat capacity is based on the assumption that the vibration is purely quantum and the rotation is purely classical.) One of the useful approaches to quantum molecular systems is the use of path integral simulations. However, heat capacity, which is the dispersion of energy, is so computationally demanding that it was not feasible until the recent development of parallel computers and efficient heat capacity estimator [2]. It is for the above reasons that even the heat capacity of liquid water, which is about 1 cal/(g K) as is well known, has never been reproduced by molecular simulations without the help of theoretical approximations [3,4].

High heat capacity in the liquid state is said to be one of the anomalous properties of water. It is twice as large as that in ice I_h at the melting point. The heat capacities of other polar molecules do increase on melting but water shows a particularly large increase. This is ascribed to changes in the hydrogen bond network by the extra energy when liquid water is heated, since this factor is not available in the solid or gaseous phase. In fact, normal-mode analysis using Debye spectra reproduces the experimental values reasonably well for the heat capacity of ice I_h, while it underestimates it fatally for that of liquid water. This implies that the conformational change has a significant contribution to the heat capacity of liquid water [5].

In this paper, we report a calculation of heat capacities for three states of water—vapor, liquid water, and ice I_h—by performing path integral molecular dynamics (PIMD) simulations [6–8]. All three states are treated the same way. Using the single point charge/flexible (SPC/F) model for water molecules [9], both the intramolecular and intermolecular interactions are included, and all hydrogen and oxygen atoms are treated quantum mechanically as cyclic bead chains in a path integral representation. Our aim is to find how well this direct molecular approach works and to see if it can reproduce the experimental heat capacities of water (see Fig. 1).

In our simulations, a normal-mode description of each path integral necklace was used, and a Nosé-Hoover chain was separately coupled to each degree of freedom to generate the canonical ensemble [10]. Gas-phase simulations were performed at 250, 300, 1000, 2000, and 3000 K. Liquid water simulations were carried out at 300 K and 1.00 g/cm^3 with 256 water molecules in a cubic cell, while ice I_h simulations were undertaken at 250 K and 0.92 g/cm^3 with 300 water molecules in a parallel-piped cell. Periodic boundary conditions were applied in these condensed-phase simulations. It has been confirmed that the ice I_h structure is stable in the present PIMD simulations using the SPC/F model. The Lennard-Jones (LJ) interaction was truncated at 10.5 Å whereas the long-range correction to the LJ energy was taken into account. For the Coulomb interaction, the Ewald method was used [11]. The reversible reference system propagator algorithm (RESPA) integration scheme [12] was used to perform the calculation of the forces on their appropriate time scales [13]. The PIMD runs were carried out for 1 ns and 100 ps for gas and condensed-phase simulations, respectively. All calculations were undertaken using an originally developed molecular simulation software, MPDYN [14], which enabled efficient PIMD simulations on a 32-node xeon PC cluster. Similar simulations for the classical molecular dynamics (MD) were also carried out.

It is known that the efficiency (the statistical convergence) in evaluating the heat capacity is different between their estimators, even though these estimators ultimately give the same values for each path integral variable (the number of beads) P. Therefore the first thing we should do here is to check the efficiency of heat capacity estimators that are currently available. Figure 2 shows the accumulative average of

*Electronic address: w.shinoda@aist.go.jp

†Electronic address: shiga@koma.jaeri.go.jp

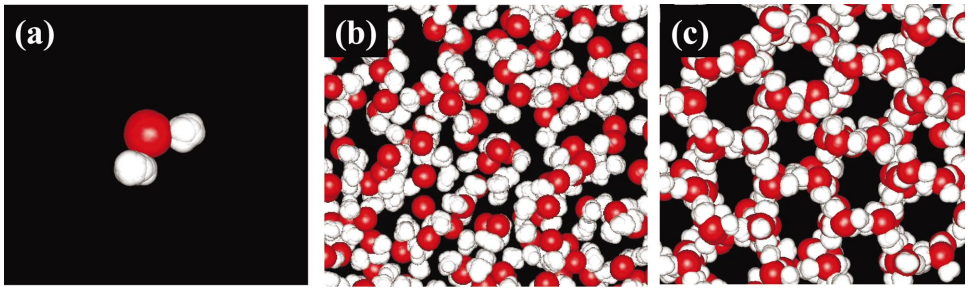

FIG. 1. (Color) Snapshots of PIMD simulations for (a) vapor, (b) liquid water, and (c) ice I_h systems for $P=128$. Superposition of red and white spheres describes a set of the bead elements for oxygen and hydrogen atoms, respectively.

heat capacity of vapor water with $P=128$ at 300 K. Among several heat capacity estimators examined here, the double centroid virial (DCV) heat capacity estimator showed the best performance in the statistical convergence. The DCV estimator is computationally demanding itself, since it requires calculation of the Hessian matrix (the whole set of the second derivative matrix of the potential). However, we can see that this is the only estimator that is efficient enough to give an accurate estimation of the heat capacity. It gives less than 2% uncertainty within 100-ps simulations. This is found to be also true for other temperatures and other phases. Thus, we decided to employ the DCV estimator with the potential cutoff at 10.5 Å as to the Hessian term.

Figures 3(a) and 3(b) show the internal energy and heat capacity of vapor water as a function of P, respectively. The internal energy monotonically increases with increasing P value and reaches its converged value at about 32 or 64. The internal energy in our SPC/F model shows reasonable agreement with a recent *ab initio* PIMD result [15] which is also plotted in the figure. We can see that the heat capacity shows a slower convergence with the P value compared with the internal energy. The heat capacity given by the classical MD simulation, which corresponds to the $P=1$ case, is about $6.0k_B$. As the P value is increased, the heat capacity value goes up until $P=4$ or 8; then, it goes back down to a converged value of $3.1k_B$, which is in excellent agreement with experimental value [16]. It is worth noting that estimation of the heat capacity needs a larger path integral variable $P \sim 128$ compared to the internal energy to obtain a converged result. This comes from the discrete imaginary time description of the quantum free energy for which the first derivative is proportional to the internal energy while the second derivative is proportional to the heat capacity.

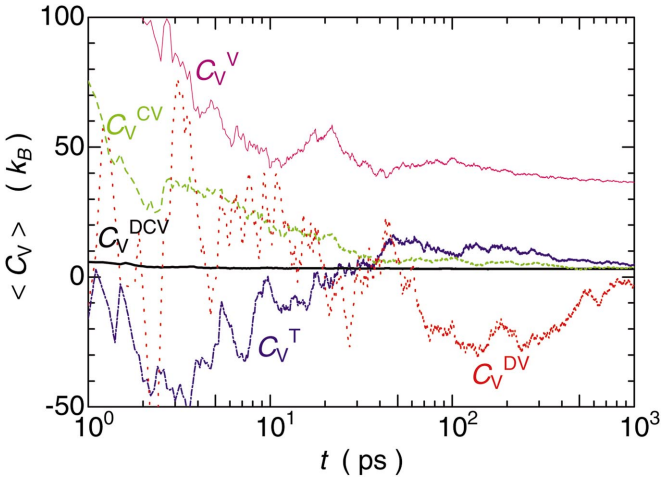

FIG. 2. (Color) Accumulative averages of the heat capacity of vapor water at 300 K. C_V^T: thermodynamic. C_V^V: virial. C_V^{CV}: centroid virial. C_V^{DV}: double virial. C_V^{DCV}: double centroid virial estimators. The notation is the same as in Ref. [2].

The temperature dependence of heat capacity for vapor water is given in Fig. 4. The heat capacity is increased from $3k_B$ to $6k_B$ as the temperature is increased. At low temperatures, the kinetic energy of the three translational and three rotational modes have a $k_B/2$ contribution, respectively, and thus the total heat capacity amounts to $3k_B$. Here, the contribution of intramolecular vibrational modes is hidden by the quantum effect. However, at higher temperature, the three vibrational modes begin to have an effect, each of them having the contribution of k_B in the high-temperature limit. This is why the heat capacity gets near to $6k_B$. The result by path integral MD is in good agreement with experimental data and the theoretical data based on rovibrational states [16,17]. We emphasize again that the quantum correction is very large at ambient temperature as to the high-frequency vibrational modes.

Quantum corrections for the energy and heat capacity are significantly large not only in the gas phase but in the condensed phase. Figure 3(c) shows a cohesive energy of condensed water as a function of P value. The cohesive energy E_{coh} is calculated as $E_{coh}=\langle E_{cond}\rangle-\langle E_{vapor}\rangle$, where $\langle E_{cond}\rangle$ and $\langle E_{vapor}\rangle$ are the internal energy of the condensed phase and vapor phase, respectively, at the same temperature. The cohesive energies in the PIMD (classical MD) simulation were calculated to be −10.9 kcal/mol (−12.6 kcal/mol) at 250 K ice and −9.7 kcal/mol (−11.2 kcal/mol) at 300 K liquid water, which were somewhat lower (higher) than the experimental values of −11.7 kcal/mol and −10.5 kcal/mol, respectively [5,18]. It should be noted here that the quantum corrections to the cohesive energies are no less than 10%. Here, our result indicating that the absolute value of the cohesive energies is reduced by a quantum effect is reasonable, since it is found experimentally that D_2O has larger cohesive energy than H_2O [5].

In Fig. 3(d), the heat capacities of liquid water and ice I_h are plotted as a function of P. Again, the heat capacity shows a slower convergence with increasing P value than does the internal energy. For ice I_h at 250 K, the heat capacity values in the PIMD calculation and the experiment are in perfect agreement, $4.1k_B$. On the other hand, for liquid water at 300 K, the PIMD value of the heat capacity, $7.0k_B$, is somewhat lower than the experimental one, $9.0k_B$. However, these results are by far better than the classical MD results, $11.0k_B$ for ice and $14.0k_B$ for liquid water.

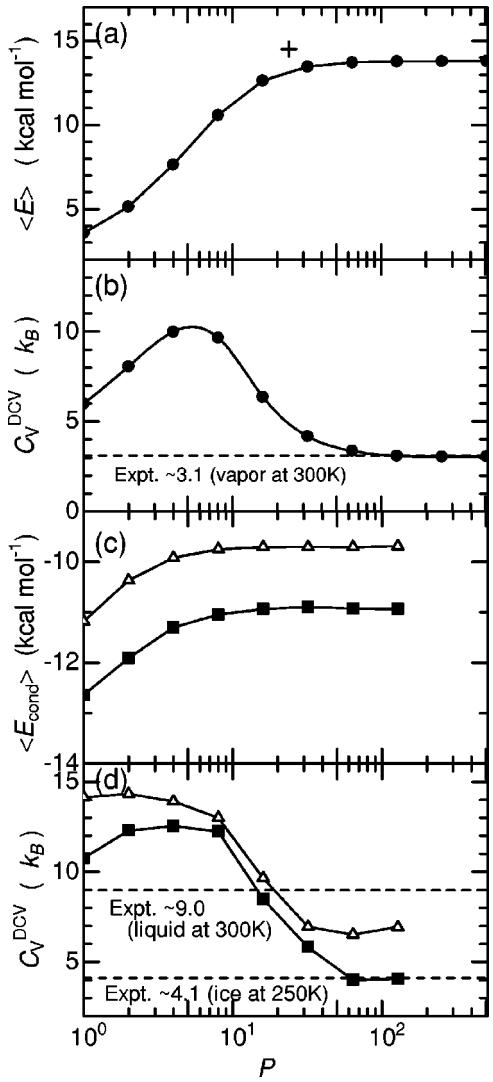

FIG. 3. Statistical convergence of internal energy and heat capacity as a function of path integral variable P. (a) The internal energy of vapor water. The cross indicates the value obtained by *ab initio* PIMD calculation at the level of the second-order Moller-Plesset perturbation theory with (6-31++G**) basis set (MP2/6-31++G**) [15]. (b) The heat capacity C_V^{DCV} of vapor water. (c) The cohesive energy $E_{\mathrm{coh}}=\langle E_{cond}\rangle-\langle E_{vapor}\rangle$ of liquid water and ice I_h. (d) The heat capacity C_V^{DCV} of liquid water and ice I_h. Open triangle: liquid water. Solid square: ice I_h. The experimental data are taken from Refs. [17,5]. The statistical errors are within the size of the symbols.

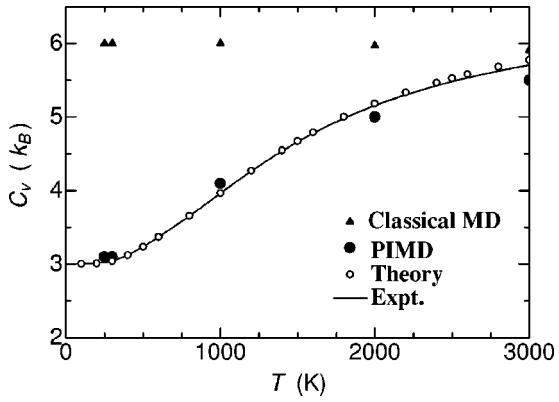

FIG. 4. Temperature dependence of the heat capacity of vapor water. The experimental and theoretical values are taken from Refs. [16,17], respectively, assuming $C_V=C_P-k_B$.

As explained above, the large heat capacity of liquid water is due to the large configurational contribution which is related to the exchange of hydrogen bonding [5]. In our PIMD simulation, the heat capacities of ice and vapor water have been reproduced very well. This means that the SPC/F potential model describes the vibrational heat capacity correctly. Therefore, the underestimation of heat capacity of liquid water should be attributable to the slight deficiency in the SPC/F model for describing hydrogen-bonded configurations. Indeed, the calculated oxygen-oxygen radial distribution function (RDF) for liquid water shows that classical MD gives a better agreement with experimental RDF [19] than does the PIMD [20]. However, we can at least say that the quantum correction for the heat capacity is very large for water at any phase. The ratio of heat capacity values between classical MD and PIMD is about 50% for liquid water at 300 K, 60% for ice I_h at 250 K, and 0–50% for vapor water depending on the temperature. We emphasize that the quantum correction has been found to be larger than $3k_B$. This means that the quantum effect cannot be explained by just neglecting intramolecular vibrational degrees of freedom. In addition, normal-mode analysis may not work for liquid water since the configurational contribution is quite large. The PIMD simulation is useful since it considers the quantum effect of rotational and translational degrees of freedom as well as vibrational degrees of freedom, and it includes the anharmonic motion and the configurational change of hydrogen bonding without any approximation except for the interatomic potential.

We have presented a quantum mechanical calculation of heat capacities of vapor (250–3000 K), liquid water (300 K), and ice I_h (250 K) by path integral molecular dynamics. The calculation reasonably converged with the simulation run of 100 ps and the imaginary time increment of $P=128$, using the DCV estimator. It has been shown that the classical simulation extremely overestimates the heat capacities in all three states, and therefore the quantum correction plays a significant role. The calculated values for vapor and ice I_h are in perfect agreement with experimental data, whereas those for liquid water are 20% lower than the experimental ones. We conclude that a slight disagreement for liquid water should be due to the limitation in the SPC/F potential model, since this model was originally parametrized by classical simulations instead of quantum simulations in order to reproduce the structural fluctuations of liquid water. However, our quantum simulation has been successful in reproducing the quality that the heat capacity of liquid water is much greater than those of ice I_h and vapor.

The DCV estimator used in this study gives the heat capacity with an error of less than $0.1k_B$. We note that heat capacity is difficult to estimate accurately just by plotting internal energies as a function of temperature. For instance, to give an estimation within the error of $0.1k_B$ for liquid water at 300 K, the energy error should be within $0.0003k_BT$

($0.003k_BT$) when the temperature points are taken every 1 (10) K. However, the energy in our path integral calculation (with the best CV energy estimator) actually had an energy error no less than $0.03k_BT$ for a 100-ps simulation. We believe that the DCV estimator works well generally for systems other than water [2].

Finally, we make a short remark on some other choices to calculate the heat capacity of water by path integral simulations. Since the DCV estimator needs a calculation of the Hessian matrix, higher-order Suzuki-Trotter expansion [21] would be helpful to reduce P value, but it is necessary to calculate third-order potential derivatives. The Hessian matrix is not easy to calculate also for the charge equilibrium-type potential [22] or rigid-body water model [23]. (The rigid-body model will not be able to evaluate the temperature dependence of water vapor since vibrational heat capacity is not taken into account.) Thus, we decided to use the simplest SPC/F model in the present work.

The authors thank Dr. H. Fukazawa at JAERI for useful discussion.

[1] A. Einstein, Ann. Phys. **22**, 180 (1907).
[2] K. R. Glaesemann and L. E. Fried, J. Chem. Phys. **117**, 3020 (2002).
[3] P. H. Berens, D. H. J. Mackay, G. M. White, and K. R. Wilson, J. Chem. Phys. **79**, 2375 (1983).
[4] M. G. Sceats and S. A. Rice, J. Chem. Phys. **72**, 3248 (1980).
[5] D. Eisenberg and W. Kauzmann, *The Structure and Properties of Water* (Clarendon, Oxford, 1969).
[6] M. E. Tuckerman, B. J. Berne, G. J. Martyna, and M. L. Klein, J. Chem. Phys. **99**, 2796 (1993); J. Cao and G. J. Martyna, *ibid.* **104**, 2028 (1996).
[7] M. Shiga, M. Tachikawa, and S. Miura, J. Chem. Phys. **115**, 9149 (2001).
[8] B. Chen, I. Ivanov, M. L. Klein, and M. Parrinello, Phys. Rev. Lett. **91**, 215503 (2004).
[9] J. Lobaugh and G. A. Voth, J. Chem. Phys. **106**, 2400 (1997).
[10] M. E. Tuckerman and A. Hughes, in *Classical and Quantum Dynamics in Condensed Phase Simulations*, edited by B. J. Berne, G. Ciccotti, and D. F. Coker (World Scientific, Singapore, 1998), p. 311.
[11] M. P. Allen and D. J. Tildesley, *Computer Simulation of Liquids* (Clarendon Press, Oxford, 1987).
[12] M. Tuckerman, G. J. Martyna, and B. J. Berne, J. Chem. Phys. **97**, 1990 (1992).
[13] For example, in case of liquid water at 300 K, the time step used for the update of reciprocal Ewald force was 1 fs, the update of short-range nonbonded force was 0.5 fs, the update of intramolecular force was 0.1 fs, and the update of the harmonic nearest-neighbor interactions along the polymer chain was 0.02 fs.
[14] W. Shinoda and M. Mikami, J. Comput. Chem. **24**, 920 (2003).
[15] M. Tachikawa and M. Shiga, J. Chem. Phys. **121**, 5985 (2004).
[16] M. W. Chase, Jr., C. A. Davies, J. R. Downey, Jr., D. J. Frurip, R. A. McDonald, and A. N. Syveraud, *JANAF Thermodynamic Tables*, 3rd ed. (American Chemical Society and American Institute of Physics for the National Bureau of Standards, New York, 1985); J. Phys. Chem. Ref. Data **14**, Suppl. 1, 1274, (1985).
[17] M. Vidler and J. Tennyson, J. Chem. Phys. **113**, 9766 (2000).
[18] The experimental cohesive energies for liquid water at 300 K and ice I_h at 250 K are evaluated using the heat of evaporation and the sublimation at 273 K together with the heat capacities around the respective states. Note that these cohesive energies are mostly dominated by the latent heat.
[19] G. Hura, J. M. Sorenson, R. M. Glaeser, and T. Head-Gordon, J. Chem. Phys. **113**, 9140 (2000).
[20] E. Schwegler, J. C. Grossman, F. Gygi, and G. Galli, J. Chem. Phys. **121**, 5400 (2004).
[21] M. Takahashi and M. Imada, J. Phys. Soc. Jpn. **53**, 963 (1984); **53**, 3765 (1984).
[22] H. A. Stern and B. J. Berne, J. Chem. Phys. **115**, 7622 (2001).
[23] M. W. Mahoney and W. L. Jorgensen, J. Chem. Phys. **115**, 10 758 (2001).